

The Effect of Embedded Super Hard Composite on the Production of Super Hard Materials: Necessity

Ojo Sunday Isaac Fayomi^{1,2}, Nduka Ekene Udoye^{1,*}, P. A. L. Anawe³, and Anthony Inegbenebor¹

¹Department of Mechanical Engineering, College of Engineering, Covenant University Ota, Ogun State, Nigeria

²Department of Chemical, Metallurgical and Materials Engineering, Tshwane University of Technology, Private Bag X680, Pretoria 0001, South Africa

³Department of Petroleum Engineering, College of Engineering, Covenant University Ota, Ogun State, Nigeria

ABSTRACT

Super alloys or high performance alloys are alloys that exhibit perfect mechanical strength and creep resistance at high temperatures, better corrosion stability and oxidation resistance. Super alloys are generally used in many industrial applications that need to operate at elevated temperatures and pressures applied static and dynamic stresses and aggressive environment due to their extraordinary mechanical properties and surface stability. They have the characteristic of an austenitic face-centered cubic crystal structure with a base alloying element of nickel, cobalt, or nickel-iron. To develop a super alloy that will be driven by the aerospace and power industries. Chemical and process innovations are the two aspect of development of decent super alloy. It is also a known fact that super alloys are developed through solid solution strengthening. In this contribution, sufficient knowledge of a close review of the impact of superalloy on corrosion, microstructure and mechanical characterization developed by composite embedded modifier agent will be examined. Their characteristics will be reviewed and tailored toward material application.

KEYWORDS: Super Alloy, Alloying Element, Solid Solution Strengthening, Composite Embedded Modifier.

1. INTRODUCTION

Nickel-base superalloys have important properties that have contributed to its major application. Higher temperature strength, oxidation resistance, excellent creep resistance, excellent fatigue resistance at elevated temperature resulted to high temperature components of gas-turbine.¹⁻³

High temperatures can withstands effects of high temperatures and alternating loading in actual service conditions in turbine disk. The quick action effect of high nickel super alloy used extensively in the gas-turbine engines was studied. The Plasticity and ductility of the super alloy can be improved by the use of high nickel. The essence of the work is to have a complete and correct performance of turbine disk that have excellent fatigue resistance, heat treatment process in addition to its composition and appropriate. The effects of heat treatment on microstructure and fatigue behaviour of nickel-base superalloys have not received thorough investigation.⁴ The mechanical property of nickel-base super alloys with superior high temperature makes them the best candidates for use in jet engines and industrial gas turbines. Operating at high temperatures

is needed in order to increase its turbine output and efficiency. High temperature strength of super alloys are sought for proper improvement.⁵ To improve hardness and strength at elevated temperatures and reduce the coefficient of expansion, an alloy of Nickel and aluminium-copper is used for the purpose.⁶

Higher temperature strength and solid solution strengthening elements have been added to generate super alloys at levels that are well above the solubility limit imposed by the solvus of the γ/γ' two-phase region. The formation of topologically close-packed phases that causes serious deterioration in creep strength will result if exposed to a very long time.^{7,8} In nuclear industry, high nickel content super alloys such as Inconel 600 are used due to their good stress corrosion cracking (SCC) resistance because of constant exposure to high temperature corrosive environment.

High chromium content nickel-based alloys have sought better primary water SCC resistance in spite of good resistance industry.⁹ A denser protective chromium oxide layer which reduce corrosion effect in both air and steam environment are formed when the chromium content tend to 30%. One of the major materials for the nuclear industry is Inconel 600 which contain 30% Cr.¹⁰ Super alloy technology remains a keystone in gas turbine materials. Characteristics exhibited by super alloy include mechanical strength, resistance to thermal creep deformation, good

* Author to whom correspondence should be addressed.

Email: nduka.udoye@covenantuniversity.edu.ng

Received: 8 February 2018

Accepted: xx Xxxx xxxx

surface stability, and resistance to corrosion or oxidation. Examples of crystal structure exhibiting face-centered cubic austenitic includes Hastelloy, Inconel, Waspaloy, Rene alloys, Haynes alloys, Incoloy, MP98T, TMS alloys, and CMSX single crystal alloys.¹¹ Super alloy development can only be achieved by using both chemical and process innovations. Super alloys produce high temperature strength by using solid solution strengthening.

Precipitation strengthening is crucial to the formation of secondary phase precipitates such as gamma prime and carbides. Aluminium and Chromium elements provide oxidation or corrosion resistance.¹² It is found mostly in turbine engines, both aerospace and marine. Mechanical properties of nickel-based super alloys of high superior temperature makes them the most used in jet engines and industrial gas turbines. To increase turbine output and efficiency, we apply higher operating temperature. The best way to improve high temperature strength of super alloy is sought.¹³

2. METHODOLOGY

2.1. Nickel-Based Super Alloys

Nickel-based alloys can be called solid solution or precipitation strengthened. Hastelloy X is a solid solution strengthened alloys used in applications requiring only modest strength. A precipitation strengthened alloy is used mostly in hot sections of gas turbine engines. Most of the known nickel-based alloys contain 10–20% Chromium, up to 8% Aluminium and Titanium, 5–10% Cobalt, and small amounts of B, Zr, and C. Mo, W, Ta, Hf, and Nb are added in small quantity. The elementary added to Ni-base super alloy can be categorized in details.¹⁴ Table I is the results of chemical composition determination of super alloy Hastelloy S obtained by wet process.

- γ formers normally divide the γ matrix
- γ' formers are elements that divide the γ' precipitate
- Carbide formers are elements that separate from the grain boundaries.

Elements that fall into the category of γ formers are Group V, VI, and VII elements such as Cobalt, Chromium, Molybdenum, tungsten and Iron. The atomic diameters of these alloys are only 3–13% different from Ni the primary matrix element. γ' Formers are from group III, IV, and V elements and include Al, Ti, Nb, Ta, Hf. The atomic diameters of these elements differ from Ni by 6–18%.¹⁵ The main carbide formers are Cr, Mo, W, Nb, Ta and Ti.

Table I. Chemical composition determination of super alloy hastelloy S obtained by wet process.¹⁵

Chemical element	Ni	Cr	Mo	Mn	Si	Fe	C	Al	B	Others
% [wt]	67.00	15.30	14.40	0.50	0.50	1.34	0.30	0.30	0.01	0.05

The primary grain boundary elements are B, C and Zr. Their atomic diameters are 21–27% different from Ni. The major phases present in most nickel super alloys are as follows.

2.2. Gamma (γ)

It is a continuous matrix that is face-centered-cubic (FCC) nickel-based austenitic phase that usually contains a high percentage of solid-solution elements such as Carbon, Cobalt, Chromium, Molybdenum, Iron, Titanium, Aluminium and Tungsten. Nickel-alloys are cooled from the melt during the formation of these materials as carbides begin to precipitate at lower temperatures γ' phase precipitates (Fig. 1). TEM micrograph shows the homogeneous distribution of the γ' phase particles in the γ matrix after quenching.¹⁶

2.3. Gamma Prime (γ')

Ni₃ (Aluminium, Titanium) is the primary strengthening phase in nickel-based super alloys. It is a unified precipitating phase that is the crystal planes of the precipitate are in registry with the gamma matrix with an ordered L1₂ (FCC) crystal structure. The close match in matrix/precipitate lattice parameter (~0–1%) combined with the chemical compatibility allows the γ' to precipitate homogeneously throughout the matrix and have long-time stability. Interestingly, the flow stress of the γ' increases with increasing temperature up to about 650 °C (1200 °F).¹⁷ In addition, γ' is quite ductile and thus imparts strength to the matrix without lowering the fracture toughness of the alloy. The major constituents that are added in amounts proportion to precipitate a high volume fraction in the matrix is Aluminium and Titanium. In addition to a given volume of precipitate, a sphere has 1.24 less surface areas than a cube, and thus is the preferred shape to minimize surface energy.¹⁸

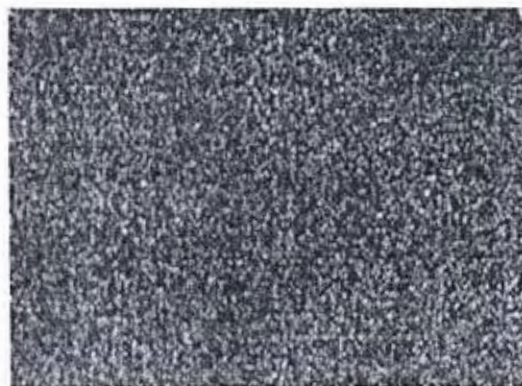


Fig. 1. TEM micrograph of γ' precipitates in the γ matrix after quenching from 1150 °C/2 h [Whittenberger].

Table II. Carbides present in different super alloys.²¹

Super alloys	Mo + W, Wt%	Primary carbides	Secondary carbides	Other carbides	Ref.
Inconel 600	1.7	MC	M ₂₃ C ₆		[7]
Nimonic 115	2.0	MC	M ₂₃ C ₆		[12]
Udimet 500	2.3	MC	M ₂₃ C ₆		[3]
Udimet 700	2.4	MC	M ₂₃ C ₆		[3]
Alloy 713C	2.6	MC	M ₂₃ C ₆		[7]
Similar to Udimet 500	5.18	MC	M ₂₃ C ₆	M ₆ C	
		(M = Ti, Mo)	(M = Cr, Mo)	(M = Mo)	

2.4. Gamma Double Prime (γ'')

They possess the composition of Ni₃Nb or Ni₃V and is used to strengthen Ni-based super alloys at lower temperatures (<650 °C) relative to γ' . The crystal structure of γ'' is body-centered tetragonal (BCT), and the phase precipitates as 60 nm by 10 nm discs with the 001 plane in γ'' parallel to the 001 family in γ . These anisotropic discs form as a result of lattice mismatch between the BCT precipitate and the FCC matrix. This lattice mismatch leads to high coherency strains which, together with order hardening, comprise the primary strengthening mechanisms. The γ'' phase is unstable above approximately 650 °C.¹⁹

2.4.1. Carbides

It is the addition of carbon which is added at levels of 0.05–0.2%, to combine with reactive and refractory elements such as titanium, tantalum, and hafnium to form carbides e.g., TIC, TAC, or HFC. They decompose and form lower carbides like M₂₃C₆ and M₆C, which develop on the grain boundaries during the heat treatment and servicing. These common carbides all have an FCC crystal structure. Results vary on whether carbides are harmful or beneficial to super alloy properties.²⁰ Carbides are beneficial by increasing rupture strength at high temperature in superalloys with grain boundaries. Table II shows different super alloys containing its Carbides.

2.5. Close-Packed Phases

These are generally undesirable, brittle phases that can form during heat treatment or service. The cell structures of these phases have close-packed atoms in layers separated by relatively large interatomic distances. The layers of close packed atoms are displaced from one another by sandwiched larger atoms, developing a characteristic called topology.²¹ These compounds have been characterized as possessing a topologically close-packed (TCP) structure. Conversely, Ni₃Al (gamma prime) is close-packed in all directions and is called geometrically close-packed (GCP). TCPs (σ , μ , Laves, etc.) usually form as plates which appear as needles on a single-plane microstructure. The plate-like structure negatively affects mechanical properties ductility and creep-rupture. Sigma appears to be the most deleterious while strength retention has been observed in some alloys containing mu and Laves.²²

3. RESULTS AND DISCUSSION

3.1. Features of the Deformation of Nickel-Based Alloys

The combination of Chromium and Cobalt with a large volume fraction of the precipitate Ni₃ (Aluminium, Titanium) and a lesser volume fraction of carbides are used in grain boundaries during nickel-based super alloy formation. The power law creep is slowed as the yield strength is raised to roughly the ultimate strength of nickel. The field of dominance is large as the diffusional flow in the super alloys is minimal. Dynamic recrystallization is anticipated at temperatures above those at which the γ' precipitate and the M₂₃C₆ and M₇C₃ carbides dissolve.²³ Figure 2 is the Nickel-10 at% chromium of grain size 100 μ m, showing data. The temperature is normalized by the melting point of pure nickel (1726 K). Figure 2 is the Nickel-10 with a grain size of 100 μ m, as cast.¹⁶ Figure 3 is the Nickel-20 at% chromium of grain size 100 μ m, showing data. The temperature is normalized by the melting point of pure nickel (1726 K).²⁴

3.1.1. Solution-Strengthened Nickel: The Nichromes (Figs. 2 and 3)

The graph of Ni-20% Cr (Fig. 3) and Ni-13.5% Cr (Fig. 4) are plotted with the temperature scale normalized to the melting temperature of pure nickel in order to facilitate direct comparison. The solidus temperature is marked on both side of the graph sheet. We calculate shear moduli from the poly-crystal data using $\mu_0 = (3/8)E_0$ to calculate Young moduli²⁵ The slow of alloy in lattice diffusion is shown in Figure 5. There is absence of data in boundary

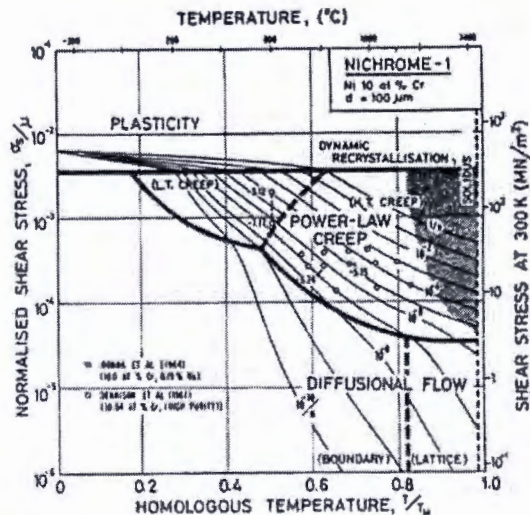


Fig. 2. Nickel-10 at% chromium of grain size 100 μ m, showing data. The temperature is normalized by the melting point of pure nickel (1726 K) [Roger].

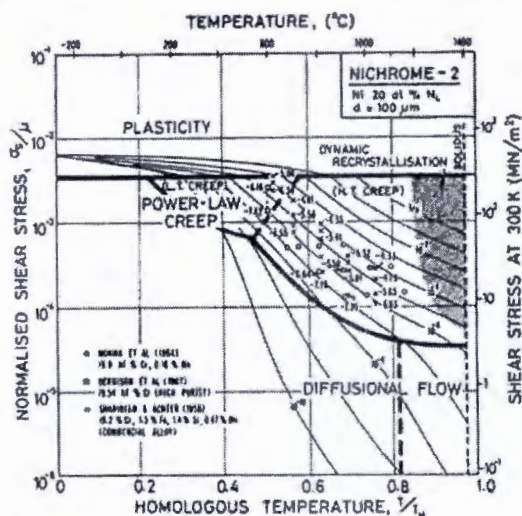


Fig. 3. Nickel-20 at% chromium of grain size 100 μm , showing data. The temperature is normalized by the melting point of pure nickel (1726 K) [Shinagawa].

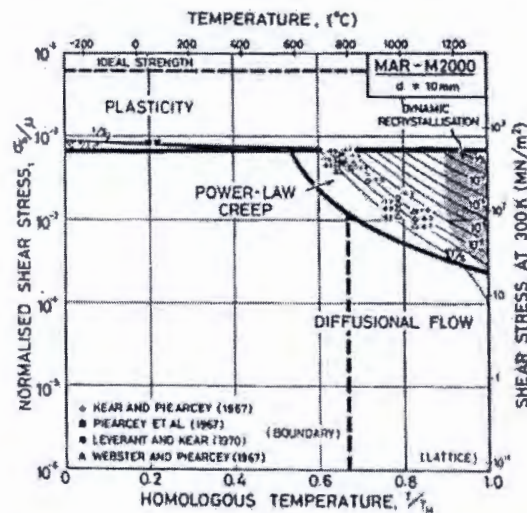


Fig. 5. MAR-M200 with a grain size of 10 μm , as cast, showing data from single-crystal samples [Roger].

or core diffusion in these alloys as depicted in Figure 5. The same activation energies is used for pure nickel.²⁶ Therefore, boundary diffusion is enhanced or reduced by the addition of a solute and dislocation in core diffusion. The rate of diffusion can be reducing by the presence of chromium. Assumption were made that boundary diffusion is reduced to take the value of D_{OB} to be 80% of the value for pure nickel.

3.2. Dispersion-Strengthened Nickel: Nickel-Thoria and Nickel-Chromium-Thoria Alloys

For pure nickel and the Ni-Cr alloys, diffusion coefficients are the same. Nickel and nichrome have equal moduli because the dispersion-strengthened alloys have a marked texture which lowers the modulus in the rolling direction of the worked state.²⁷ The grain size for the Ni-1% ThO₂ alloy ($d = 0.1 \text{ mm}$) is an approximation made from published micrographs. A larger grain size ($d = 0.2 \text{ mm}$) was used for Ni-Cr-ThO₂ alloys because the smaller value incorrectly places much of the creep data in the diffusional flow field the high observed stress component of between 5 and 7 indicates power-law creep. There are no reports of diffusional flow in thoriated nickel and nichromes. The field was calculated using the diffusion coefficients for pure nickel and for the nichromes described earlier. The threshold stress shown in Figure 4 is based on creep data for Cu-Al₂O₃ and Au-Al₂O₃ alloys.⁹ Table III is the nominal composition of MAR-M200 in wt%.²⁸

Alloying lowers the melting point to 1600 K and raises the shear modulus lightly to 80 GN/m² compared with pure nickel. We take the coefficient for lattice and boundary diffusion to be the same as those for high-alloy nichrome due to Lack of complete data. The dispersion of Ni₃(Al, Ti), superimposed on the heavy solid-solution strengthening of the tungsten and Chromium. It gives MAR-M200 and alloys yield strength comparable with

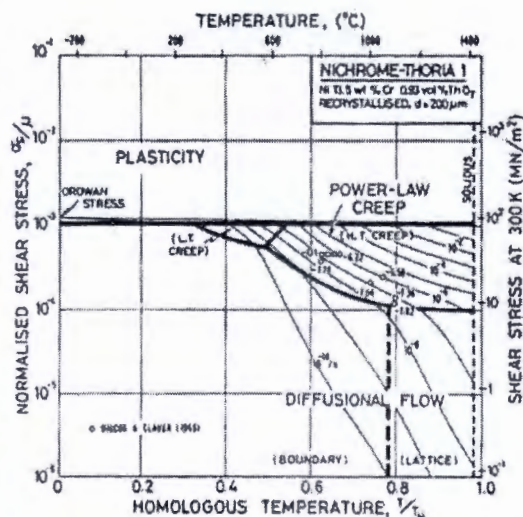


Fig. 4. Nickel 13.5 wt% Cr-0.93 vol.% ThO₂ of grain size 200 μm , recrystallized [Shinagawa].

Table III. Nominal composition of MAR-M200 in wt%.⁹

Al	Ti	W	Cr	Nb	Co	C	B	Zr	Ni
5.0	2.0	12.5	9.0	1.0	10.0	0.15	0.015	0.05	Bal.

the ultimate strength of pure nickel, although it is less dependent on temperature.²⁹ Precipitation strengthening and solution hardening have raised the yield line, and have reduced drastically the size of the power-law creep field. They also change the rate of diffusional flow due to incomplete experimental data for MAR-M200, we have made the assumption that it occurs at the same rate as it would in Ni-20% Cr alloy. The γ' phase dissolves at a slightly higher temperature, the grain boundary carbides do so also ($M_{23}C_6$ at 1040 to 1095 °C; M_7C_3 at 1095 to 1150 °C¹⁰).

We are not aware of observations of dynamic recrystallization in MAR-M200, but above 1000 °C the γ' phase dissolves, and at a slightly higher temperature the grain boundary carbides do so also ($M_{23}C_6$ at 1040 to 1095 °C; M_7C_3 at 1095 to 1150 °C¹⁰). This means that above 0.9 T_M the alloy is a solid solution and if the data cited earlier for solid solutions can be used as a guide, we would expect dynamic recrystallization.

4. CONCLUSION

In conclusion, super alloys with grain boundaries containing carbides are beneficial by increasing rupture strength at high temperature. TCPs are potentially damaging for two reasons: they tie up gamma and gamma prime strengthening elements in a non-useful form. This reduces creep strength and act as crack initiators because of their brittle nature. This lattice mismatch leads to high coherency strains which, together with order hardening, comprise the primary strengthening mechanisms. The gamma double prime phase is unstable above approximately 650 °C. Gamma γ during the formation of these materials, as the Ni-alloys are cooled from the melt, carbides begin to precipitate at even lower temperatures gamma phase. Precipitation strengthening and solution hardening have raised the yield line and have reduced drastically the size of the power-law creep field. They also change the rate of diffusional flow^{13,14} though, because of lack of experimental data for MAR-200. We concluded that it occurs at the same rate as it would in Ni-20% Cr alloy. We are not aware of observations of dynamic recrystallization in MAR-M200, but above 1000 °C the γ' phase dissolves, and at a slightly higher temperature the grain boundary carbides do so also $M_{23}C_6$ at 1040 to 1095 °C; M_7C_3 at 1095 to 1150 °C; This means that above 0.9 T_M the alloy is a solid solution, and if the data cited earlier for solid solutions can be used as a guide, we would expect dynamic recrystallization. The shaded field is based on this reasoning. Precipitation strengthening and solution hardening have raised the yield line, and have reduced drastically the size of the power-law creep field.

Acknowledgments: The authors will like to acknowledge the support of Covenant University, Ota, Nigeria for open access.

References and Notes

1. W. Harrison, M. Whittaker, and S. Williams, Recent advances in creep modelling of the nickel base superalloy, alloy 720Li. *Materials* 6, 1118 (2013).
2. D. G. L. Prakash, M. J. Walsh, D. Maclachlan, and A. M. Korsunsky, Crack growth micro-mechanisms in the IN718 alloy under the combined influence of fatigue, creep and oxidation. *Int. J. Fatigue* 31, 1966 (2009).
3. M. V. Acharya and G. E. Fuchs, The effect of long-term thermal exposures on the microstructure and properties of CMSX-10 single crystal Ni-base superalloys. *Mater. Sci. Eng. A* 381, 143 (2004).
4. Z. Peng, Z. Qiang, C. Gang, Q. Heyong, and W. Chuanjie, Effect of heat treatment process on microstructure and fatigue behavior of a nickel-base superalloy. *Open Access Material* 1, 1996 (2015).
5. S. Atsushi, The effects of ruthenium on the phase stability of fourth generation Ni-base single crystal superalloys. *Elsevier Scripta Materialia* 54, 1679 (2006).
6. O. S. I. Fayomi, N. E. Udoe, and A. P. I. Popoola, Effect of alloying element on the integrity and functionality of aluminium based alloy. *Intech Open Access Journal* 12 (2017).
7. D. F. Darolia and R. D. Lahrman, Field Formation of Topologically Closed Packed Phases in Nickel Base Single Crystal Superalloys, edited by Reichman, et al., TMS, Warren Dale (PA) (1988), p. 255.
8. J. B. Ferguson and H. F. Lopez, Oxidation products of inconel alloys 600 and 690 in pressurized water reactor environments and their role in intergranular stress corrosion cracking. *Metals Mater. Trans.* 8, 2471 (2006).
9. Das physical aspects of process control in selective laser sintering of metals. *Adv. Eng. Mater.* 5, 701 (2003).
10. S. C. Roger, *The Super Alloys: Fundamentals and Applications*, Cambridge University Press, Cambridge, UK (2006).
11. L. Klein, Y. Shen, M. S. Killian, and S. Virtanen, Effect of B and Cr on the high temperature oxidation behaviour of novel γ/γ' strengthened co-base super alloys. *Corrosion Science* 53, 271 (2011).
12. K. Shinagawa, O. Toshihiro, and K. Ishida, Ductility enhancement by boron addition in Co-Al-W high temperature. *Alloys Scripta Materialia* 6, 15 (2009).
13. C. T. Sims, *A History of Super Alloy Metallurgy for Super Alloy Metallurgists* (1984), pp. 399–419.
14. B. A. Wilcox and A. H. Clauer, Creep of dispersion-strengthened nickel-chromium alloys. *Met. Sci. J.* 3, 26 (1969).
15. H. Gleiter and B. Chalmers, High-angle grain boundaries. *Program Material Science* 16, 93 (1972).
16. J. P. Dennison, R. J. Llewellyn, and B. Wilshire, The creep and failure properties of some nickel-chromium alloys at 600 °C. *J. Inst. Met.* 95, 115 (1967).
17. G. A. Webster and B. J. Pearcey, An interpretation of the effects of stress and temperature on the creep properties of a nickel-base super alloy. *Met. Sci. J.* 1, 97 (1967).
18. J. D. Whittenberger, Elevated temperature mechanical properties and residual tensile properties of two cast super alloys and several nickel-base oxide dispersion strengthened alloys. *Met. Trans.* 12, 193 (1981).
19. C. Roger, *The Super Alloys: Fundamentals and Applications*, Cambridge University Press (2006).
20. L. Klein, Y. Shen, M. S. Killian, and S. Virtanen, Effect of B and Cr on the high temperature oxidation behaviour of novel γ/γ' strengthened co-base super alloys. *Corrosion Science* 53, 720 (2011).
21. M. Durand-Charre, *The Microstructure of Super Alloys*, Science Publisher, Amsterdam, Gordon and Breach (1997), p. 1.
22. C. J. Boehlert, D. S. Dickmann, and N. C. Eisinger, *Metallurgical Material Transition A* 1, 27 (2006).
23. E. L. Shoemaker and J. R. Crum, *The Solution to Corrosion Problems in Wet Limestone FGD*, Special Metal, p. 21.
24. P. M. Mignaneli, N. G. Jones, and E. J. Pickering, Gamma-gamma, prime gamma double prime dual super lattice super alloys. *Scripta Materialia* 136, 136 (2017).